# The numerical solution of Richards equation: a simple method adaptable in a parallel computing

N. Egidi[a], E. Gioia[b], P. Maponi[a] and L. Spadoni[a]

[a]School of Sciences and Tecnology, University of Camerino
[b]Department of Life Sciences and the Environment, Marche Polytechnic University

**ARTICLE HISTORY**
Compiled December 14, 2017

**ABSTRACT**
Numerical simulation models of water flow in variably saturated soils are important tools in water resource management, assessment of water-related disaster and agriculture. Richards equation is one of the most used models for the fluid flow simulation into porous media. This is a partial differential equation whose analytical solution is only possible under a number of restrictive assumptions. Therefore the deriviation of efficient numerical schemes for its approximated solution has to be computed by discretization methods. We propose a numerical procedure considering a simplified linearization scheme that makes it adaptable to parallel computing. A comparison in computational performances with other three numerical procedures is detailed for a large numerical experiments, including the assessment of the landslide hazard in real areas. We prove the efficiency of the simplified numerical procedure by comparing the results we obtained with a parallel code.

**KEYWORDS**
Soil moisture; Richards equation; hydrological modelling; landslide hazard; slope stability analysis.

**AMS CLASSIFICATION**
65M06, 76S05, 65M22

## 1. Introduction

Numerical simulation models for water flow in unsaturated soils are important tools in hydrology, meteorology, agronomy, environmental protection, and other soil-related disciplines. An increasingly important issue related to the soil moisture dynamics is the soil pollution, which consists of altering the chemical and geological balance caused by the transmission and transport of pollutants into the soil, compromising quality of freshwater [28, 30, 32]. The soil moisture dynamics can give also important inputs to the efficient use of water resources, avoiding unnecessary irrigations in agriculture and silviculture activities [29]. The soil water fluxes play a key role in the water-related risk analysis: rainfall-induced landslides or floods cause property

CONTACT N. Egidi Email: nadaniela.egidi@unicam.it
CONTACT E. Gioia Email: e.gioia@staff.univpm.it
CONTACT P. Maponi Email: pierluigi.maponi@unicam.it
CONTACT L. Spadoni Email: lorenza.spadoni@unicam.it

damage and pose a threat to life. For this reason, accurate prediction systems in areas prone to water-related events constitute an important objective in Civil Protection. An efficient warning system for the quantitative evaluation of the landslide hazard should combine the weather predictions with the dynamics of soil moisture and a slope stability model [4, 5], [34, 41].

The Richards equation [35] is one of the main tool for the fluid flow simulation into porous media. It has been introduced by Richards, on the basis of the Darcy's law and mass continuity law [33]: thanks to the combination of these two principles, Richards obtained a non linear partial differential equation, defining the water flow both in the saturated and unsaturated porous media.

Richards equation can be given by different formulations: the head form, the moisture content form and the mixed form are the most usual versions, but also other transformed forms of the equation are possible [18, 22]. Nevertheless the Richards equation cannot be solved by analytical methods: in particular, its strong non-linearity is due to the soil hydraulic functions which relate the water content and the hydraulic conductivity with the hydraulic head [31, 39]. An approximated solution has to be computed by discretization methods. Strategies for the numerical solution of Richards equation depends on the approximation techniques for the space derivatives and the time derivatives and the solution method for the nonlinear system of discretization equations. Several numerical routines have been already proposed in the scientific literature. The use of finite difference [14, 16, 17] or finite element [9, 13, 25] methods to approximate the space derivatives in Richards equation are the dominant approaches. These methods are usually applied on a fixed spatial grid, although an adaptive approach has been examined as well [1]. The standard time derivative approximation method is the Euler approach [42]. Picard [20], modified Picard [22] and Newton [26] methods are the most frequently used to deal with the nonlinearity of the Richards equation. Regardeless of the method used, the linearization of Richards equation yields to a system of linear equations, which is typically solved by using direct methods in one dimensional problem [2], while iterative approaches must be considered for large linear systems arising form three-dimensional problems [38].

The numerical solution of Richards equation is still a subject of intense research, mainly, for the reduction of the computation time needed to achieve accurate results in heterogeneous soils [6, 7, 27] and/or large geographical areas [8]. Furthermore, real-world applications require the joint analysis of the soil moisture dynamics with complementary processes, such as energy balance, geochemical reactions and rain runoff, which make the computational problem of solving the Richards equation even more complex. So, in the near future, the current computational tools for the solution of Richards equation have to be extended to much larger computational domains (in terms of spatial size as well as of physical processes analysed) and they must be adapted to be implemented in High Performance Computing (HPC) codes.

Another difficulty in Richards equation is the efficient acquisition of model parameters. Actually, this is a quite common situation to all the mathematical models of complex phenomena; however, in this particular case, it is a very crucial issue since it depends on the weather data and on the geotechnical features of the soil. Weather is usually acquired by proper stations on the territory or by satellite measurements. Soil features are mainly characterized by the granulometry, which can be used to identify the textural class of the soil studied among a number of possible classes and it can be obtained by direct measurements and/or general geomorphological features of the territory. So, both sets of these data are difficult to get with high spatial resolution and accuracy. Unfortunately the lack of information can limit the

successfull application of Richards equation to real-world problems, so a precise sensitivity analysis for such a model should be provided in order to obtain reliable results.
The purpose of this paper is to present a simple numerical scheme which is able to solve the three dimensional Richards equation and readily adptable to parallel computing. In order to test its efficiency, we compare this scheme with other three numerical procedures developed for the solution of Richards equation; these four procedures differ for the discretization scheme and/or for the linearization approach as well as for the numerical solution of the linearized equations. The performance of the numerical schemes are investigated in twelve homogeneous types of soil. We compare these procedures in the application of landslide hazard evaluation on three geographical areas where soils with heterogeneous types are present. At the end, in order to demonstrate the potentially contribute that the simple procedure can bring to the efficiency of the numerical solution of Richards equation, we provide its results after using a simple parallel implementation.

The remaining part of the paper is organized as follows. Section 2 briefly describes the Richards equation. In Section 3, we present four numerical procedures, which are based on the finite difference method and the finite element method. Section 4 provides the first numerical experiment comparing the performance of the procedures on a water infiltration problem where twelve types of soil are considered. In Section 5, an application of the Richards equation to the landslide hazard evaluation problem is proposed and the corresponding results are provided for three geographical areas. Section 6 provides the results of the simple numerical procedure after using a parallel implementation concerning the three geographical areas and some soil types. In section 7 we give some conclusions and future development of this work.

## 2. The soil moisture dynamics

For the convenience of the reader, we describe the main features of the soil material and the model for the soil moisture dynamics, that is the Richards equation. This equation is one of the main tool for the simulation of fluid flow in porous media, and it is presented in the following sections. In particular in Section 2.1 we define the most important soil physical characteristics. Section 2.2 describes the Richards equation.

### *2.1. The soil physical characteristics*

The soil is a porous medium consisting of a solid matrix characterized by microscopic cavities that can be filled by air or by water [19].
The volume of the pore space or equivalently the volume of voids, is denoted with the symbol $V_v$. The ratio between the volume of water $V_w$ contained in the volume $V$ and the volume of voids $V_v$ is called the *degree of saturations* $S$, so:

$$S = \frac{V_w}{V_v}. \tag{1}$$

The amount of water present in a porus medium can be described also by the *water content* $\theta$ which is defined as

$$\theta = \frac{V_w}{V}. \tag{2}$$

The complete saturation condition ($S = 1$) is very difficult to achieve: this fact is due to the presence of small air bubbles or blind pores [19]. We denote with $\theta_s$ the *saturated water content*, that is the maximum water content that can be achived in a soil. Also the absolute absence of water in the soil ($S = 0$) is an extreme situation difficult to reach; we denote with $\theta_r$ the *residual water content*, that is the minimum water content that we can find in the soil.
The ratio of the volume of voids to the total volume $V$ is usually called the *porosity* and it is denoted with the symbol $n_\epsilon$, so

$$n_\epsilon = \frac{V_v}{V}. \tag{3}$$

The water present in a porous medium is subject to a great variety of forces; however, due to the difficulty in describing this complex system, it is preferred to refer to the energy [33] of water particles: in particular, at each point, this is the sum of the kinetic energy (related to the velocity of the fluid) and of the potential energy (linked to the position of the point in the gravitational field and the pressure of the fluid). Because of the modest velocities characterizing the usual infiltration and redistribution phenomena in soil, the kinetic energy is neglected so that the total energy coincides with the potential component and is expressed in terms of the *hydraulic head*, that is

$$h = \psi + z, \tag{4}$$

where $z$ is the height compared to an arbitrary level reference and $\psi$ is the *pressure head*. It is worth noticed that $h$ is expressed in units of length since the potential component is considered in term of elevation, see [33] for details.

### *2.2. Richards equation*

According to Richards [35], the soil water flow is modeled by combining Darcy's law and mass conservation equation, yielding the following equation

$$\Big(C(\psi) + S_s\frac{\theta(\psi)}{n_\epsilon}\Big)\frac{\partial h}{\partial t} =$$

$$= \frac{\partial}{\partial x}\Big(K(\psi)\frac{\partial h}{\partial x}\Big) + \frac{\partial}{\partial y}\Big(K(\psi)\frac{\partial h}{\partial y}\Big) + \frac{\partial}{\partial z}\Big(K(\psi)\frac{\partial h}{\partial z}\Big) + W - ET, \tag{5}$$

where $C(\psi) = \frac{d\theta}{d\psi}$ is the specific capillary capacity, $S_s$ is the storage coefficient, $K(\psi)$ is the hydraulic conductivity, $W$ is the recharge and it is related to the rate of precipitation, $ET$ is the evapotraspiration and it represents the loss of water due to the

evaporation of bare soils and traspiration of plants (it can be estimated by Penman-Monteith formula [3]). Equation (5) can be used for describing water movement in saturated and unsaturated porous media.
The functions $\theta(\psi)$ and $K(\psi)$ can be supplied by empirical formulas: the Van Genuchten model [39] is probably the most used in scientific computation applications because of its formulation by smooth functions. A usual version of this model can be written as follows:

$$\frac{\theta - \theta_r}{\theta_s - \theta_r} = \begin{cases} \left(\frac{1}{1+|\alpha\psi|^n}\right)^m & \text{if } \psi < 0 \\ 1 & \text{if } \psi \geq 0, \end{cases} \tag{6}$$

where $\alpha$ is the reciprocal value of $\psi_0$, i.e. the air entry point [39], $\theta_r$ is the residual water content, $\theta_s$ is the saturated water content, $n$ and $m$ are empirical parameters depending on the soil, which must satisfy the following restriction

$$m = 1 - \frac{1}{n}. \tag{7}$$

The relative hydraulic conductivity function can be derived from $\theta$, with the following formula:

$$K(\theta) = K_s \Big(\frac{\theta - \theta_r}{\theta_s - \theta_r}\Big)^{\frac{1}{2}} \Big(1 - \Big[1 - \Big(\frac{\theta - \theta_r}{\theta_s - \theta_r}\Big)^{\frac{1}{m}}\Big]^m\Big)^2. \tag{8}$$

By using (6), we can expressed (8) in the following form:

$$K(\psi) = \begin{cases} K_s[1 - (\alpha\psi)^n]^{-m/2}\Big[1 - \left(\frac{|\alpha\psi|^n}{1+|\alpha\psi|^n}\right)^m\Big]^2 & \text{if } \psi < 0 \\ K_s & \text{if } \psi \geq 0, \end{cases} \tag{9}$$

where $K_s$ is the value of the permeability when the soil is saturated.
The various hydraulic parameters, e.g., $\alpha$, $\theta_r$, $\theta_s$, $n$, $K_s$, are related to the pore size distribution and pore geometry, so they ultimately depend on the soil type and can be determined experimentally by specific laboratory tests. Table 1 shows typical values of $\alpha$, $\theta_r$, $\theta_s$, $n$, $K_s$ related to twelve usual types of soils which are classified on the base of the percentage of clay (Cl), silt (Si), sand (Sa), coarse-sand (Csa), and gravel (Gr) in the soil [15, 23, 36, 40].

Equation (5) is a non linear differential equation, whose solution $h$ is a function of spatial variables $(x, y, z) \in \Omega$ and time variable $t$. The computation of this solution requires knowledge of the initial distribution of the hydraulic head $h$ inside the space domain $\Omega \subset R^3$. Moreover, it requires the knowledge of appropriate boundary conditions along the domain boundary $\partial\Omega$: specified hydraulic head (Dirichlet type) and specified flux (Neumann type) are the most commonly used in soil-related applications, see [33] for details.

**Table 1.**

| | Parameters | | | | | |
|---|---|---|---|---|---|---|
| Type | Description | $\theta_r$ | $\theta_s$ | $\alpha[1/m]$ | n | $K_s[m/s]$ |
| CLAY | Cl> 75% | 0.11 | 0.48 | 1.33 | 1.31 | 1.00E-08 |
| SILTY CLAY | Cl> 50% Si>Sa | 0.11 | 0.48 | 1.46 | 1.33 | 4.00E-07 |
| CLAYEY SILT | Si> 50% Cl>Sa | 0.08 | 0.47 | 1.00 | 1.45 | 4.17E-07 |
| SILT | Si> 75% | 0.05 | 0.49 | 0.66 | 1.65 | 1.00E-06 |
| SANDY SILT | Si> 50% Sa>Cl | 0.04 | 0.45 | 1.05 | 1.53 | 1.89E-06 |
| SILTY SAND | Sa> 50% Si>Cl | 0.06 | 0.40 | 2.78 | 1.39 | 5.05E-06 |
| SAND | Sa> 75% | 0.05 | 0.39 | 3.36 | 2.11 | 5.83E-05 |
| CLAYEY SAND | Sa> 50% Cl>Si | 0.08 | 0.40 | 2.14 | 1.36 | 2.83E-06 |
| SANDY CLAY | Cl> 50% Sa>Si | 0.11 | 0.43 | 2.73 | 1.24 | 1.72E-06 |
| SAND-SILT-CLAY | Sa=Si=Cl | 0.08 | 0.45 | 2.49 | 1.42 | 2.75E-06 |
| COARSE SAND | CSa> 75% | 0.02 | 0.36 | 15.85 | 2.91 | 1.00E-03 |
| GRAVEL | Gr> 75% | 0.02 | 0.36 | 15.85 | 2.91 | 5.01E-03 |

Different type of grain sizes and the corresponding parameters $\theta_r$, $\theta_s$, $\alpha$, $n$, $K_{sat}$.

## 3. The discretization schemes and their implementation

We define four procedures for the numerical solution of Richards equation: such procedures differ for the discretization scheme, for the linearization approach and/or for the solution of the linearized equations. In particular, we take into account two numerical methods for the discretization in the space domain that are the finite difference method and the finite element method, described in Section 3.1 and in Section 3.2, respectively. These methods yield to a first order non-linear initial-value problem in the time variable, analyzed in Section 3.3, whose solution can be found by applying an iterative procedure together with a linearization strategy to deal with such a non linear problem. In Section 3.3 we sescribe the different linearization strategies taken into account.

### *3.1. The Finite difference approximation*

A popular method to solve (5) is the finite difference scheme with central difference quotients for the space derivatives:

$$\left(C^n_{i,j,k} + S_s \frac{\theta^n_{i,j,k}}{n_\epsilon}\right)\frac{\partial h^n}{\partial t}(x_i, y_j, z_k) =$$

$$= \frac{1}{(\Delta x)^2}\Big[K^n_{i+1/2,j,k}(h^n_{i+1,j,k} - h^n_{i,j,k}) - K^n_{i-1/2,j,k}(h^n_{i,j,k} - h^n_{i-1,j,k})\Big] +$$

$$+ \frac{1}{(\Delta y)^2}\Big[K^n_{i,j+1/2,k}(h^n_{i,j+1,k} - h^n_{i,j,k}) - K^n_{i,j-1/2,k}(h^n_{i,j,k} - h^n_{i,j-1,k})\Big] +$$

$$+ \frac{1}{(\Delta z)^2}\Big[K^n_{i,j,k+1/2}(h^n_{i,j,k+1} - h^n_{i,j,k}) - K^n_{i,j,k-1/2}(h^n_{i,j,k} - h^n_{i,j,k-1})\Big] + W^n_{i,j,k} - ET^n_{i,j,k}, \quad (10)$$

where $\Delta x$, $\Delta y$, $\Delta z$ are the discretization steps in the $x$, $y$ and $z$ direction, respectively; $h^n_{i,j,k}$ denote the approximate value of $h$ in the generic grid point $(x_i, y_j, z_k)$ at time

$t_n$; a similar notation is used for $C$, $K$ and $\theta$. Note that values of discrete function $K$ at non integer indices are obtained by the average of the same function at integer indices.

### 3.2. Finite element approximation

We suppose $\partial\Omega = \partial\Omega^D \cup \partial\Omega^N$, where we prescribed a Dirichlet boundary condition on $\partial\Omega^D$ and a Neumann boundary condition on $\partial\Omega^N$. We consider the Galerkin method [9], that is based on the weak formulation of the Richards equation (5):

$$\int_\Omega w\Big(C(\psi) + S_s \frac{\theta(\psi)}{n_\epsilon}\Big)\frac{\partial h}{\partial t}\ d\underline{x} + \int_\Omega \nabla w \cdot [K(\psi)\nabla h]\ d\underline{x}$$

$$-\int_\Omega w(W - ET)\ d\underline{x} + \int_{\partial\Omega^N} w q_h\ ds(\underline{x}) = 0, \qquad \forall w \in H^1{}_0(\Omega), \tag{11}$$

where $q_h = [K(\psi)\cdot\nabla h]\cdot\nu$, $\nu$ is the outward normal vector of $\partial\Omega^N$, and $H_0^1(\Omega)$ is the space of square integrable functions $w$ having square integrable derivative defined almost everywhere, and such that $w(x) = 0$, $x \in \partial\Omega^D$.
Solution $h$ is approximated by a function $\tilde{h}(\underline{x}, t) \approx \sum_{j=1}^{N_p} N_j(x)h_j(t)$ where $N_j(x), x \in \Omega$, $j = 1, 2, \ldots, M_p$ is a basis of functions and $h_j(t)$ are unknown coefficients to be determined; in particular, this basis is usually defined by piece-wise polynomial functions $N_i$ having a small support $\Omega_i$ with respect to the whole domain $\Omega$. For semplicity we suppose that an homogeneous Dirichlet boundary condition is prescribed on $\partial\Omega^D$. The Galerkin method considers the weighting function $w$ equal to the representation functions, i.e. $N_i$, so formula (11) becomes

$$\sum_{j=1}^{M_p}\frac{\partial h_i}{\partial t}\int_{\Omega_i\cap\Omega_j} N_i\Big(\tilde{C} + S_s\frac{\tilde{\theta}}{n_\epsilon}\Big)\ N_j d\underline{x} + \sum_{j=1}^{M_p}\int_{\Omega_i\cap\Omega_j}\tilde{K}\nabla N_i\cdot\nabla N_j\ d\underline{x}$$

$$-\int_{\Omega_i} N_i(W - ET)d\underline{x} + \int_{\partial\Omega_i{}^N} N_i q_h ds(d\underline{x}) = 0$$

$$i = 1, 2, \ldots, M_p; \tag{12}$$

where $\tilde{C} = C(\tilde{h}(\underline{x}))$; a similar notation is used for $\tilde{\theta}$ and $\tilde{K}$.

### 3.3. Time discretization schemes

We consider a partition $t_n = n\Delta t$ of the time domain $[0, T_0]$, $n = 0, \ldots N$, where $\Delta t > 0$ is the time step. We observe that both (10) and (12), coupled with the initial value of $h$, represent an initial-value problem in the time variable, so we can formally rewrite these systems as

$$\frac{\partial \underline{h}^n}{\partial t} = F(\underline{h}^n, t_n), \tag{13}$$

where $\underline{h}^n$ is the vector of the unknowns at time $t = t_n$, $F(\underline{h}^n, t_n)$ is a non linear vector function.
For the numerical solution of (13), we consider the single step methods [12] that can be expressed in their generalized form

$$\underline{h}^{n+1} = \underline{h}^n + \Delta t[(1-\lambda)F(\underline{h}^n, t_n) + \lambda F(\underline{h}^{n+1}, t_{n+1})], \tag{14}$$

where $\lambda$ is a weighting factor, $0 \leq \lambda \leq 1$.
The case $\lambda = 0$ is called explicit Euler method, the case $\lambda = \frac{1}{2}$ is called Crank Nicolson method while the case $\lambda = 1$ is called implicit Euler method.

### *3.4. Linearization tecniques*

At each time $t_n$, the numerical solution of nonlinear system (14) must be computed by an approximation method. For this problem, we propose a simple iterative procedure. Let $\underline{h}^{n+1,0}$ be an initial solution of (14) at time $t_{n+1}$; we define $\underline{h}^{n+1,r}$ for $r = 1, 2, \ldots R$ by the following recursive procedure:

$$\underline{h}^{n+1,r} = \underline{h}^n + \Delta t[(1-\lambda)F(\underline{h}^n, t_n) + \lambda F(\underline{h}^{n+1,r-1}, t_{n+1})], \tag{15}$$

where, given an appropriate tolerance *toll*, $R$ is the first iterate satisfying:

$$\left|\left|\underline{h}^{n+1,r} - \underline{h}^{n+1,r-1}\right|\right|_\infty < toll. \tag{16}$$

Note that, the initial guess $h^{n+1,0}$ is computed by the explicit Euler method and at the end of the iterative process we define

$$\underline{h}^{n+1} = \underline{h}^{n+1,R}. \tag{17}$$

Other linearization methods used to solve (14) are *Picard linearization scheme* and *Newton scheme* [24].
The iterative procedure (16) provides a very simple linearization scheme, so we can expect only a limited efficacy of this procedure. However, it is very interesting from the computational point view, in fact formula (15) does not require the solution of a linear system. So, in addition to its low computational cost, this procedure can be also efficiently implemented in parallel codes in fact, the successive estimates $\underline{h}^{n+1,r}$ in equation (15) depends only on the solution of the previous time step $\underline{h}^n$ and the previous estimates of the new time step $\underline{h}^{n+1,r-1}$.

### *3.5. The procedures*

We define four numerical procedures for the solution of Richards equation. These procedures are obtained by combining the previously described approximation approaches in order to compare their efficiency.

**Procedure 1.** The finite difference method is used for space discretization; the solution of the system (14) is computed by the Crank-Nicolson method togheter with the linearization scheme (15).

**Procedure 2.** The finite difference method is used for space discretization; the solution of the system (14) is computed by the implicit Euler method togheter with the Picard linearization scheme and the solution of the corresponding linearized systems is obtainded by the multifrontal method, that is a direct method based on a sparse variant of Gaussian elimination, see [10] for a detailed presentation of this method.

**Procedure 3.** The finite difference method is used for space discretization; the solution of the system (14) is carried out by implicit Euler method togheter with the Picard linearization scheme and the solution of the corresponding linearized systems is obtainded by means of the preconditioned conjugate gradient method.

**Procedure 4.** The Galerkin finite element method [9] is used for space discretization; the solution of the system (14) is carried out by the implicit Euler method togheter with the Picard linearization scheme and the solution of the corrispondind linearized systems is obtainded by means of the preconditioned conjugate gradient method.

## 4. Numerical experiments

We investigate the behavior of the four numerical procedures proposed in Section 3.5 in a range of twelve different soil types. In all the simulations we consider the same spatial domain $\Omega_1 = [0, L_x] \times [0, L_y] \times [0, L_z]$, where $L_x = 90m$, $L_y = 50m$ and $L_z = 4m$ and the same time period of 10 days. Table 1 shows the values of $\alpha$, $\theta_r$, $\theta_s$, $n$, $K_s$ for the considered soil types with respect to the Van Genucthen model, see [15] for details. At time $t = 0$ all the simulations start from a uniform saturation equal to 30% and the time period is characterized by a precipitation rate of 100 $mm/day$. At the boundary of $\Omega_1$ we impose the zero normal flow condition.
In all the simulations we used a constant time step $\Delta t$ equal to 15 minutes except for Procedure 1, when coarse sand and gravel type are considered: in these cases, the convergence of the linearization method requires the reduction of the time step by a factor 1000, compromising the efficiency of the procedure. In fact the elapsed CPU time for Procedure 1 is about 4 $s$ for all the soils, but it grows at 11 minutes when coarse sand and gravel type are considered. The elapsed CPU time relative to Procedure 2, Procedure 3, Procedure 4 is about 8 $s$, 5 $s$ and 4 minutes, respectively, in all the soil types. We tested our simulations using Window PCs with 16 GB of RAM and Intel Core i7, CPU 3.4 GHz.
Table 4 shows a comparison between the soil water content computed by the four numerical procedures on the basis of the $RE(1, j)$, i.e. the relative error in the 2-norm between the solution computed by Procedure 1 and the one computed by Procedure $j$ ($j = 2, 3, 4$) at the end of the simulation period. We observe that, despite its simple structure, Procedure 1 performs quite well in a large number of soils, providing also good agreement with the results obtained by the other procedures with the exception of the coarse sand soil, in fact, the solution for this soil is affected by a high the relative error when compared with all the other procedures.
Procedures 1 and 2 are implemented with a FORTRAN program; for the multifrontal method in Procedure 2, we used implementation provided by routine MA57 available in the HSL software library [21]. Procedure 3 is implemented by using the software package Variably Saturated Flow Process (VSF) for MODFLOW 2005, see [37] for details. Procedure 4 is implemented by software package FEFLOW, see [9] for details.

**Table 2.**

| | $RE(1,2)$ | $RE(1,3)$ | $RE(1,4)$ |
|---|---|---|---|
| CLAY | 0.0311 | 0.000122 | 0.0808 |
| SILTY CLAY | 0.00405 | 0.00262 | 0.0368 |
| CLAYEY SILT | 0.000468 | 0.0257 | 0.0147 |
| SILT | 0.000590 | 0.00304 | 0.0631 |
| SANDY SILT | 0.00130 | 0.00290 | 0.0114 |
| SILTY SAND | 0.00305 | 0.00368 | 0.0387 |
| SAND | 0.000389 | 0.0399 | 0.0565 |
| CLAYEY SAND | 0.000997 | 0.00151 | 0.0709 |
| SANDY CLAY | 0.00438 | 0.000564 | 0.0360 |
| SAND-SILT-CLAY1 | 0.000211 | 0.00174 | 0.0348 |
| COARSE SAND | 0.6143 | 0.54 | 0.614 |
| GRAVEL | 0.0103 | 0.0665 | 0.0299 |

Comparison between the solution computed by Procedure 1 and the other procedures for the twelve soil types described in Table 1.

## 5. A landslide hazard application

We consider the application of Richards equation for a quantitative evaluation of the landslide hazard.
The majority of slope instabilities are caused by particular weather conditions, such as heavy rainfall or rapid snow melting, and are strongly associated with the pore water pressure of soil that rapidly varies during rainfall (infiltration process) and after the rainfall (redistribution process). These processes cause the increase in pore saturation which in turn increases the pore pressure with the consequent reduction of the effective stress of the soil that may trigger the slope failure. For this reason, the solution of Richards equation integrated with a slope stability model can be an effective procedure to assess the slope failure directly from weather data. The efficiency of such a procedure depends on the quality and the quantity of available weather data and geomorphological information. The spatial scale usually ranges from large areas of thousands of square kilometers, to small areas encompassing a single landslide. However, any reliable procedure for landslide hazard evaluation should be accurately adapted to the particular geographical areas taken into account; in fact this is a complex system depending on several geological, biological and climate factors but also on social aspect like the land use.

The landslide hazard problem is usually formulated in terms of the $Safety$ $Factor$, which is given by the ratio between the forces that prevent the slope from failing and those that bring the slope to collapse. So, the safety factor gives an immediate way to compute a landslide hazard index: a value larger than 1 indicates stable conditions, a value smaller than 1 indicates unstable conditions.
The $Infinite$ $Slope$ $Model$ [11] is probably the easiest method for the computation of the safety factor $F$, that is given by the following formula:

$$F = \frac{C + (z\gamma - z_w\gamma_w)\cos^2\beta\tan\phi}{z\gamma\sin\beta\cos\beta}, \tag{18}$$

where $C$ is the effective cohesion, $\gamma$ is the unit weight of the soil, $\phi$ is the angle of internal friction, $\gamma_w$ is the unit weight of water; $z$ is the depth of the failure surface, $z_w$ is the height of the watertable above failure surface, $\beta$ is the slope of the inclined surface. Table 3 shows the values of the geotechnical parameters $C$, $\gamma$, $\phi$ relative to

**Table 3.**

| | Parameters | | |
|---|---|---|---|
| Type | $C$ $[kPa]$ | $\gamma[kN/m^3]$ | $\phi$[degree] |
| CLAY | 20.60 | 20.00 | 23.3 |
| SILTY CLAY | 12.77 | 18.14 | 18.2 |
| CLAYEY SILT | 7.69 | 16.33 | 21.1 |
| SILT | 6.25 | 18.50 | 30.0 |
| SANDY SILT | 8.95 | 15.68 | 30.5 |
| SILTY SAND | 2.00 | 17.95 | 33.5 |
| SAND | 0.99 | 16.38 | 35.0 |
| CLAYEY SAND | 11.25 | 20.70 | 32.8 |
| SANDY CLAY | 3.50 | 19.75 | 28.8 |
| SAND-SILT-CLAY | 4.88 | 18.30 | 24.5 |
| COARSE SAND | 3.75 | 19.07 | 29.0 |
| GRAVEL | 1.23 | 19.00 | 37.0 |

Different type of grain sizes and the corresponding parameters $C$, $\gamma$, $\phi$.

the twelve different types of soils we definied in Section 2.2.

The combination of the Infinite Slope Model (18) and the soil water flow, i.e. Richards equation, allows the landslide hazard evaluation directly from weather data. In particular, the solution of Richards equation (5) is used to obtained information about $z_w$ in formula (18) that is given by the thickness of the saturated layer above the failure surface; while the depth $z$ coincide with the nodes of the domain and it was computed increasing by 1 $m$ for each node below the ground surface.
In the following, we consider a numerical experiment where the landslide hazard index is computed on three geographical areas. In this experiment the soil moisture dynamics is computed by Procedures 1, 2, 3.
The first test area measures 11.69 $km^2$ and is located in the mid part of the Esino river basin (central part of Italy) where a landslide occurred on March 2015. This is representative a area due to its landslide susceptibility; moreover, previous geological and geotechnical studies have provided all the required geomorphological information: the soil is mostly characterized by clay, silty clay, silty sand, sand, clayey sand and sandy clay. This area is given by steep slope as we can see in Figure 1a that is a graphical representation of the slope values on the geographical area taken into account. The proposed experiment considers the test area during the three months before the landslide event (December/6/2014 to March/6/2015); in this observation period, 258 $mm$ of rain fell. At time $t = 0$ the initial saturation is chosen equal to 70% and we imposed the zero normal flow condition at the boundary of the spatial domain. Figure 1b shows a graphical representation of the safety factor values evaluated at time $t = 0$ of the simulation: a nearly red zone is an unstable region ($F < 1$); a nearly green zone is a stable region ($F > 1$). The numerical solution of Richards equation is computed by both Procedure 1 and Procedure 2; in these simulations we consider a temporal discretization $\Delta t = 15$ minutes and a spatial discretization $\Delta C = 9.32m$, $\Delta R = 12.85m$, $\Delta V = 1m$, the number of nodes is equal to 466955. The relative error in the 2-norm between the soil moisture computed by Procedure 1 and the one computed by Procedure 2 at the end of the simulation period is 0.00285. Procedure 1 takes 278 minutes to complete the simulation, while Procedure 2 takes 656 minutes. Figure 2a and 2b show a graphical representation of the safety factor values concerning the last day of the simulation and carried on by Procedure 1 and Procedure 2 respectively. Figure 2c shows a graphical representation of the water

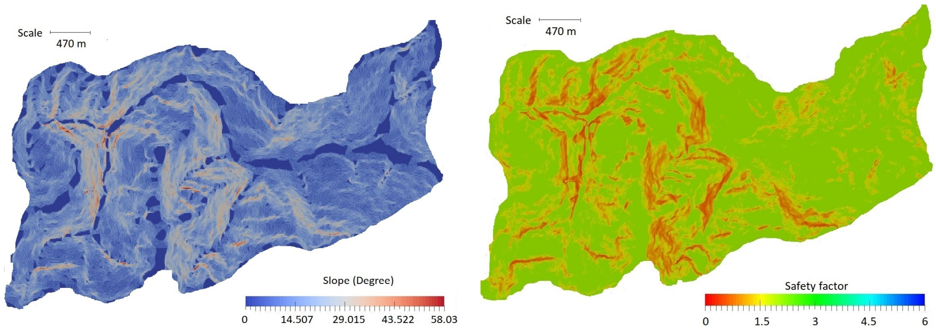


(a) Italian test area: graphical representation of the slope values.

(b) Italian test area: graphical representation of the safety factor at time $t = 0$ of the simulation.

**Figure 1.** Graphical representation of the slope values and the safety factor at time $t = 0$ concerning Italian test area.

table depth evaluated at time $t = 0$ of the simulation.
The second experiment considers a small area of Panagopoula (Greece) of about 1.5 $km^2$, where the soil is mostly characterized by clay, sand, clayey sand and sandy silt clay. Also in this case we considers a time period of 10 days characterized by a precipitation rate of 100 $mm/days$. At time $t = 0$ the initial saturation is equal to 30% and the zero normal flow condition is imposed at the boundary of the domain. The safety factor values evaluated at time $t = 0$ are represented in Figure 3b and the values of the slope of the test area are represented in Figure 3a.
Also in this case, the numerical solution of Richards equation is computed by Procedure 1 and Procedure 2, in these simulations we consider a temporal discretization $\Delta t = 15$ minutes and a spatial discretization $\Delta C = 4.63m$, $\Delta R = 5.91m$, $\Delta V = 1m$; the number of nodes is equal to 391067. The relative error in the 2-norm between the soil moisture computed by Procedure 1 and the one computed by Procedure 2 at the end of the simulation period is 0.00170. Procedure 1 takes 50 minutes to complete the simulation, while Procedure 2 takes 187 minutes. Figure 4a and 4b show a graphical representation of the safety factor values concerning the last day of the simulation and carried on by Procedure 1 and Procedure 2 respectively. Figure 4c shows a graphical representation of the water table depth evaluated at time $t = 0$ of the simulation.
The third test area considers the Smolyan Lakes, its size is about 7.4 $km^2$, it is located northwest of the town of Smolyan (Bulgaria), and the soil is completely characterized by gravel. In this case we study the test area during a time period of 10 days characterized by a precipitation rate of 100 $mm/day$. At time $t = 0$ the initial saturation is equal to 20%, and the zero normal flow condition is imposed at the boundary of the domain. The safety factor evaluated at time $t = 0$ and the values of the slope of the test area are represented in Figure 5b and in Figure 5a respectively.
The numerical solution of Richards equation is computed by Procedure 1 and Procedure 3; in these simulations we consider a temporal discretization $\Delta t = 15$ minutes and a spatial discretization $\Delta C = 4.7m$, $\Delta R = 6.2m$, $\Delta V = 1m$; the number of nodes is equal to 582428. Procedure 3 takes 10 minutes to complete the simulation, while Procedure 1 breaks down. Figure 6a shows a graphical representation of the safety factor values concerning the last day of the simulation relative to the Procedure 3 for the soil moisture dynamics. Figure 6b shows a graphical representation of the water table depth evaluated at time $t = 0$ of the simulation.
Procedure 1 provides a high efficient tool for the solution of Richards equation in

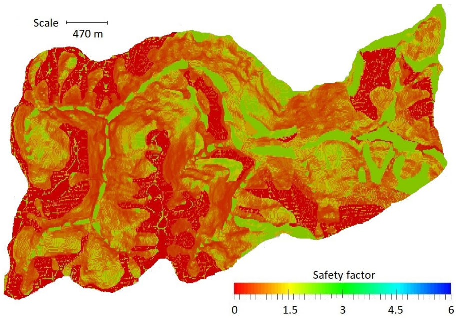


(a) Procedure 1: graphical representation of the safety factor at time $t = 10$ of the simulation concerning Italian test area.

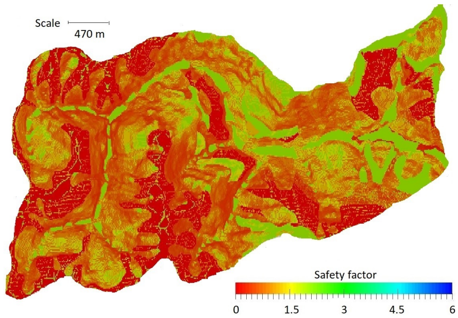


(b) Procedure 2: graphical representation of the safety factor at time $t = 10$ of the simulation concerning Italian test area.

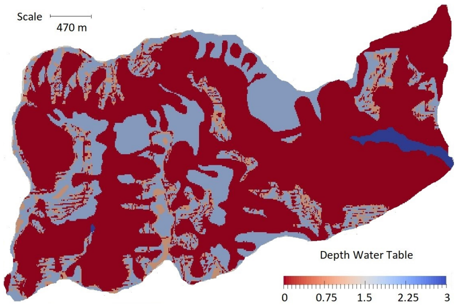


(c) Italian area: graphical representation of the water table depth at time $t = 10$ of the simulation.

**Figure 2.** Italian test area: comparison between Procedure 1 and Procedure 2 in the evaluation of the safety factor and graphical representation the water table depth at time $t = 10$

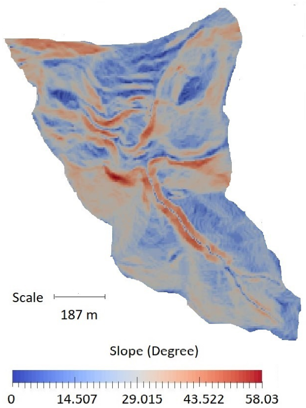


(a) Greek area: graphical representation of the slope values.

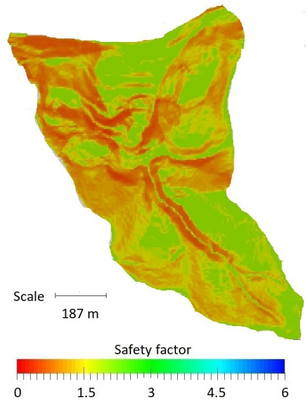


(b) Greek area: graphical representation of the safety factor at time $t = 0$ of the simulation.

**Figure 3.** Graphical representation of the slope values and the safety factor at time $t = 0$ concerning the Greek area.

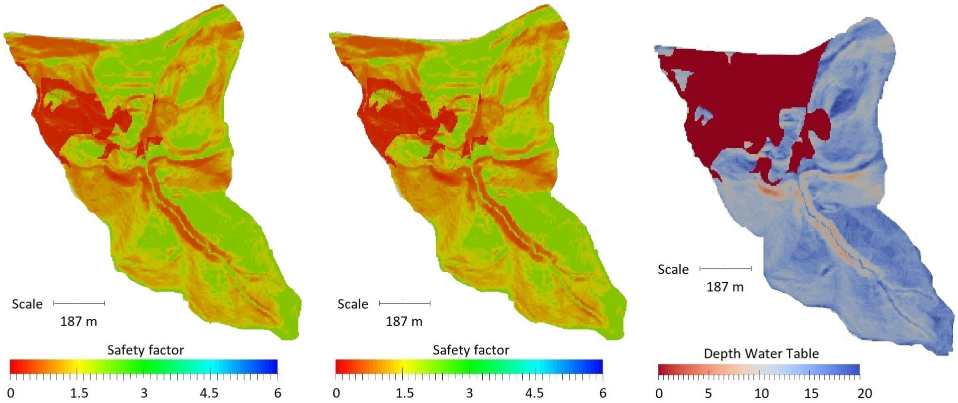


(a) Procedure 1: graphical representation of the safety factor at time $t = 10$ of the simulation concerning Greek area

(b) Procedure 2: graphical representation of the safety factor at time $t = 10$ of the simulation concerning Greek area

(c) Greek area: graphical representation of the depth of the water table at time $t = 10$ of the simulation.

**Figure 4.** Greek test area: comparison between Procedure 1 and Procedure 2 in the evaluation of the safety factor and graphical representation of the depth of the water table at time $t = 10$.

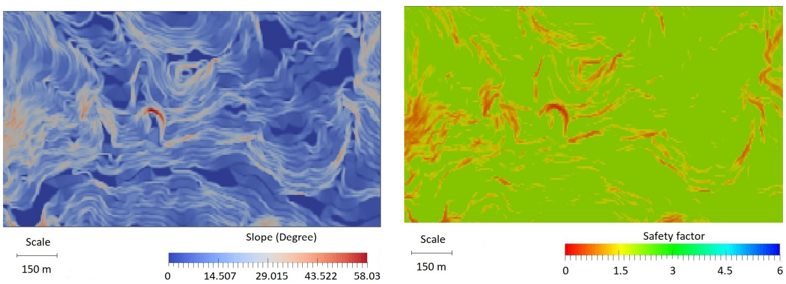


(a) Bulgarian area: graphical representation of the slope values.

(b) Bulgarian area: graphical representation of the safety factor at time $t = 0$ of the simulation.

**Figure 5.** Graphical representation of the slope values and the safety factor at time $t = 0$ concerning the Bugarian area.

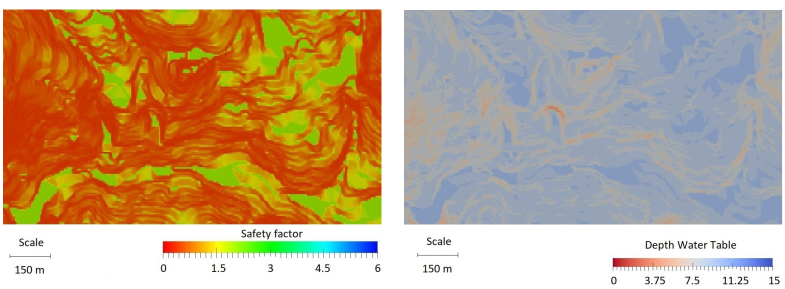


(a) Bulgarian area: graphical representation of the safety factor at time $t = 10$ of the simulation.

(b) Bulgarian area: graphical representation of the water table depth at time $t = 10$ of the simulation.

**Figure 6.** Graphical representation of the depth of the water table and the safety at time $t = 10$ concerning the Bugarian area.

both Italian area and Greek area: in this case, its computational cost is significantly lower than the one of Procedure 2, which is not efficient even in the computation of the numerical solution of Richards equation for the Bulgarian area, where it takes 61 minutes to complete the simulation. Procedure 1 does not provide satisfactory results for Bulgarian test area. This confirms the numerical results of section 4, where we have already oberved the inability of Procedure 1 to deal with soils of type coarse sand and gravel, for which we should deserve a more detailed analysis. We can suppose that Procedure 1, if implemented in parallel codes, could obtain computational costs efficient as well as the ones of Process 3, which performs quite well even in the computation of the numerical solution of Richards equation for the Italian and Greek area, where it takes 63 and 17 minutes respectively.

## 6. Code parallelization

## 7. Conclusions

The water movement in soil systems is described by Richards equation, a non linear partial differential equation whose solution has several application fields. Appropriate numerical methods for the approximation of such a solution can be taken into account: in this paper, we described four different procedures to solve Richards equations. They are compared in a range of twelve soil types, in terms of the accuracy in the solution and the execution time. These procedures are also tested in the landslide hazard evaluation on three geographical area with heterogeneous soil: in this case, the soil moisture is combined with the Infinity Slope Model to assess the safety factor directly from the weather data. Results show that Procedure 1 is unable to deal with two types of soil: coarse sand and gravel type, so it breaks down when we compute the landslide hazard evaluation in the Bulgarian test area. On the contrary, Procedure 1 seems to provide acceptable results in a very efficient way in all the other soil types. We note that these are quite surprising results, in fact they show that the very simple algorithm is able to deal with a large number of soils.

Procedure 1 does not require the solution of a linear system and this is an important aspect providing high efficiency in the solution of large scale problems. Moreover, this feature made sure that we get very efficient implementation by parallel computing codes........ So, despite its simplicity, Procedure 1 provides a concrete computational tool able to numerically solve Richards equation on large geographical areas, which is the pressing demand of several important applications, like natural hazard evaluation, water resource analysis and weather forecast.

Procedure 1 deserves a more detailed analysis in order to overcome the difficulty to deal with gravel and coarse sand soils. New linearization algorithms and relaxation techniques will be the first tools employed to enhance Procedure 1.

## 8. Acknowledgment

This activity was partially supported by LANDSLIDE (ECO/SUB/2014/693902), an European project co-financed by the Directorate General Humanitarian Aid and Civil

Protection of the European Commission.
We owe many thanks for providing free of charge the software package MODFLOW and demo version of FEFLOW, respectively.

## References

[1] L.M. Abriola and J.R. Lang, *Self-adaptive hierarchic finite element solution of the one-dimensional unsaturated flow equation*, International Journal for Numerical Methods in Fluids 10 (1990), pp. 227–246.

[2] M.B. Allen and C.L. Murphy, *A finite-element collocation method for variably saturated flow in two space dimensions*, Water Resources Research 22 (1986), pp. 1537–1542.

[3] R.G. Allen, L.S. Pereira, D. Raes, M. Smith, *et al.*, *Crop evapotranspiration-guidelines for computing crop water requirements-fao irrigation and drainage paper 56*, FAO, Rome 300 (1998), p. D05109.

[4] R.L. Baum and J.W. Godt, *Early warning of rainfall-induced shallow landslides and debris flows in the usa*, Landslides 7 (2010), pp. 259–272.

[5] R.L. Baum, W.Z. Savage, and J.W. Godt, *Trigrs-a fortran program for transient rainfall infiltration and grid-based regional slope-stability analysis, version 2.0*, Tech. Rep., US Geological Survey, 2008.

[6] H. Berninger, R. Kornhuber, and O. Sander, *Fast and robust numerical solution of the richards equation in homogeneous soil*, SIAM Journal on Numerical Analysis 49 (2011), pp. 2576–2597.

[7] H. Berninger, M. Ohlberger, O. Sander, and K. Smetana, *Unsaturated subsurface flow with surface water and nonlinear in-and outflow conditions*, Mathematical Models and Methods in Applied Sciences 24 (2014), pp. 901–936.

[8] G. Capparelli and P. Versace, *Flair and sushi: two mathematical models for early warning of landslides induced by rainfall*, Landslides 8 (2011), pp. 67–79.

[9] H.J. Diersch, *FEFLOW: finite element modeling of flow, mass and heat transport in porous and fractured media*, Springer Science & Business Media, 2013.

[10] I.S. Duff, *Ma57—a code for the solution of sparse symmetric definite and indefinite systems*, ACM Transactions on Mathematical Software (TOMS) 30 (2004), pp. 118–144.

[11] J.M. Duncan, S.G. Wright, and T.L. Brandon, *Soil strength and slope stability*, John Wiley & Sons, 2014.

[12] I. Faragó, *Convergence and stability constant of the theta-method*, Applications of Mathematics 2013 (2013), pp. 42–51.

[13] P.A. Forsyth, Y. Wu, and K. Pruess, *Robust numerical methods for saturated-unsaturated flow with dry initial conditions in heterogeneous media*, Advances in Water Resources 18 (1995), pp. 25–38.

[14] R.A. Freeze, *Three-dimensional, transient, saturated-unsaturated flow in a groundwater basin*, Water Resources Research 7 (1971), pp. 347–366.

[15] E. Gioia, G. Speranza, M. Ferretti, J.W. Godt, R.L. Baum, and F. Marincioni, *Application of a process-based shallow landslide hazard model over a broad area in central italy*, Landslides 13 (2016), pp. 1197–1214.

[16] R. Hanks and S. Bowers, *Numerical solution of the moisture flow equation for infiltration into layered soils*, Soil Science Society of America Journal 26 (1962), pp. 530–534.

[17] A.W. Harbaugh, *MODFLOW-2005, the US Geological Survey modular ground-water model: the ground-water flow process*, US Department of the Interior, US Geological Survey Reston, VA, USA, 2005.

[18] R. Haverkamp, M. Vauclin, J. Touma, P. Wierenga, and G. Vachaud, *A comparison of numerical simulation models for one-dimensional infiltration*, Soil Science Society of America Journal 41 (1977), pp. 285–294.

[19] D. Hillel, *Environmental soil physics: Fundamentals, applications, and environmental con-*

*siderations*, Academic press, 1998.

[20] R. Hills, I. Porro, D. Hudson, and P. Wierenga, *Modeling one-dimensional infiltration into very dry soils: 1. model development and evaluation*, Water Resources Research 25 (1989), pp. 1259–1269.

[21] HSL, *Ma57 sparse symmetric system: multifrontal method*, http://www.hsl.rl.ac.uk/catalogue/ma57.html (2001). Available on line.

[22] M.R. Kirkland, R. Hills, and P. Wierenga, *Algorithms for solving richards' equation for variably saturated soils*, Water Resources Research 28 (1992), pp. 2049–2058.

[23] C.P. Kumar and S. Mittal, *Determination of soil hydraulic properties in a part of hindon river catchment using soilprop software* 16 (2010).

[24] F. Lehmann and P. Ackerer, *Comparison of iterative methods for improved solutions of the fluid flow equation in partially saturated porous media*, Transport in Porous Media 31 (1998), pp. 275–292.

[25] C. Li, *A simplified newton iteration method with linear finite elements for transient unsaturated flow*, Water resources research 29 (1993), pp. 965–971.

[26] C. Li, *A simplified newton iteration method with linear finite elements for transient unsaturated flow*, Water resources research 29 (1993), pp. 965–971.

[27] N. Li, X. Yue, and L. Ren, *Numerical homogenization of the richards equation for unsaturated water flow through heterogeneous soils*, Water Resources Research 52 (2016), pp. 8500–8525.

[28] W. Ma and X.y. You, *Numerical simulation of plant–microbial remediation for petroleum-polluted soil*, Soil and Sediment Contamination: An International Journal 25 (2016), pp. 727–738.

[29] J.C. Mailhol, P. Ruelle, and Z. Popova, *Simulation of furrow irrigation practices (sofip): a field-scale modelling of water management and crop yield for furrow irrigation*, Irrigation science 24 (2005), pp. 37–48.

[30] T. Miao and T. Pan, *A multiphysics model for evaluating electrokinetic remediation of nuclear waste-contaminated soils*, Water, Air, & Soil Pollution 226 (2015), p. 77.

[31] Y. Mualem, *A new model for predicting the hydraulic conductivity of unsaturated porous media*, Water resources research 12 (1976), pp. 513–522.

[32] T. Pan and T. Miao, *Contamination of roadside soils by runoff pollutants: a numerical study*, Transportation Geotechnics 2 (2015), pp. 1–9.

[33] G.F. Pinder and M.A. Celia, *Subsurface hydrology*, John Wiley & Sons, 2006.

[34] M. Polarski, *Distributed rainfall–runoff model incorporating channel extension and gridded digital maps*, Hydrological processes 11 (1997), pp. 1–11.

[35] L.A. Richards, *Capillary conduction of liquids through porous mediums*, Physics 1 (1931), pp. 318–333.

[36] G.M.H. ROGER B. CLAPP, *Empirical equations for some soil hydraulic properties* 78 (1978).

[37] R.B. Thoms, R.L. Johnson, and R.W. Healy, *User's guide to the variably saturated flow (vsf) process to modflow*, Tech. Rep., 2006.

[38] M.D. Tocci, C. Kelley, C.T. Miller, and C.E. Kees, *Inexact newton methods and the method of lines for solving richards' equation in two space dimensions*, Computational Geosciences 2 (1998), pp. 291–309.

[39] M.T. Van Genuchten, *A closed-form equation for predicting the hydraulic conductivity of unsaturated soils*, Soil science society of America journal 44 (1980), pp. 892–898.

[40] K.E.S. W. J. Rawls D. L. Brakiensek, *Estimation of soil water property* 25 (2010).

[41] S. YU SCHREIDER, A. Jakeman, and A. Pittock, *Modelling rainfall-runoff from large catchment to basin scale: The goulburn valley, victoria*, Hydrological Processes 10 (1996), pp. 863–876.

[42] R.L. Zarba, E. Bouloutas, and M. Celia, *General mass-conservative numerical solution for the unsaturated flow equation*, Water Resources Research WRERAQ 26 (1990), pp. 1483–1496.